

Performance of a Pilot-Scale Wet Electrostatic Precipitator for the Control of Sulfuric Acid Mist and Fine Particulates

Sang Hyun Jeong¹, Sung Hoon Shim¹, Dong Keun Song¹, Won Seok Hong¹,
Jeong Hee Hong², Sang-Sup Lee^{3*}

¹Environmental and Energy Research Division, Korea Institute of Machinery and Materials,
171 Jang-dong Yuseong-gu, Daejeon, 305-343 Republic of Korea

²KC Cottrell, 160-1 Dongkyo-dong Mapo-gu, Seoul, 121-898 Republic of Korea

³Department of Environmental Engineering, Chungbuk National University,
410 Sungbong-ro Heungduk-gu, Cheongju, 361-763 Republic of Korea

Received: 10 February 2012

Accepted: 18 September 2012

Abstract

Because sulfuric acid mist and fine particulates such as PM_{2.5} are difficult to capture in typical dry electrostatic precipitators (ESPs), using a wet ESP is a viable option for the control of sulfuric acid mist and fine particulates in a flue gas. In this study, bench-scale tests were first conducted to find acceptable methods for achieving uniform water distribution and effective discharge. Based on the bench-scale results, a pilot-scale wESP was designed and constructed. The pilot-scale wESP demonstrated good performance on the removal of sulfuric acid mist and fine particulates.

Keywords: wet electrostatic precipitator, sulfuric acid mist, sulfur trioxide, fine particulate

Introduction

During the combustion of sulfur-containing fossil fuels, sulfur trioxide (SO₃) is formed by the oxidation of sulfur dioxide (SO₂). SO₃ has undesirable impacts, such as with plume opacity and corrosion [1-3]. SO₃ rapidly takes up water to form sulfuric acid (H₂SO₄) at temperatures below the acid dew point. The sulfuric acid aerosols scatter light efficiently, so the emission of such aerosols can result in a visible plume. Condensed sulfuric acid can be deposited anywhere downstream in a utility plant, causing corrosion problems on steel surfaces [4-6]. Because sulfuric acid mist is difficult to capture in typical dry electrostatic precipitators, wet electrostatic precipitators (wESP) have been proposed for the effective capture of acid aerosols [7]. Because

acid aerosols are usually soluble in water, they may be easily removed by the flow of water in a wESP. However, unless the flushing liquid is uniformly distributed over the surface, some collected particles will remain on the surface without being flushed. Although atomization or spraying liquid may improve water distribution over the surface, this can produce water mists in the gas flow. These aqueous mists will have a conductive path to ground due to their higher conductivity than the typical flue gas [7]. Although many studies have been conducted for effective control of various pollutants using a wESP, bench-scale systems were used for most of these studies [8-12]. Therefore, the objectives of this study are successful scale-up from a bench-scale to a pilot-scale wESP system and effective control of sulfuric acid mist and fine particulates using the pilot-scale wESP. Several methods were tested here to obtain a uniform distribution of flushing water over the collection plate

*e-mail: slee@chungbuk.ac.kr

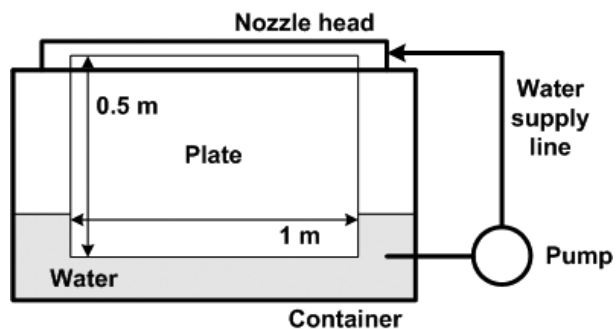


Fig. 1. Schematic of the wetting test setup.

surface. Various electrodes also were tested for effective discharge using a bench-scale test setup. The bench-scale test results were applied to the design of the pilot-scale wESP. The pilot-scale wESP was tested for its performance on the removal of sulfuric acid mist and fine particulates to examine the possibility of using it for the control of combustion flue gases.

Experimental Procedures

Wetting Test Setup

An experimental system was designed and constructed to test water distribution on the collector surface. As shown in the schematic of the experimental setup in Fig. 1, a 0.5-m-high and 1-m-wide metal plate was mounted vertically, and a nozzle head was located on the top of the plate to flush the surface simulating operation of wESP. The flushed water was re-circulated to the nozzle through a pump, and its flow rate was controlled constantly by a valve. Two kinds of water nozzles, a pinhole nozzle (P) and a flat nozzle (F), were tested. The pinhole nozzle was divided into two types depending on the method used for tip grinding. The first nozzle (P₁) has a constant diameter of 0.5 mm through the pinhole, but the other nozzle (P₂) has a bigger diameter at its tip than the body diameter, as shown in Fig. 2.

Discharge Test Setup

Different shapes of electrodes were examined. Fig. 3 shows the tested electrodes:

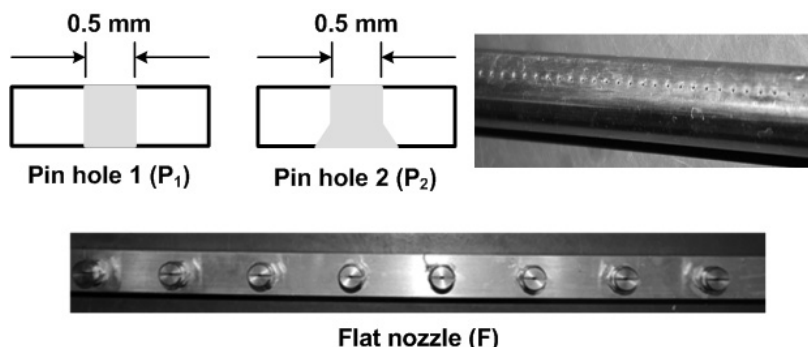


Fig. 2. Tested water nozzles.

- (1) a rod electrode with cross-arranged needles
- (2) a sharp-edged electrode
- (3) a flat-edged electrode

Similar to the wetting test setup, a 1-m-high and 1.2-m-wide plate was mounted as a collector, and a nozzle head was located on the top of the plate. Discharge electrodes were installed 150 mm distant from the collector, and a high voltage was supplied to the electrode. A schematic of the discharge test setup is shown in Fig. 4.

Pilot-Scale Wet Electrostatic Precipitator

A pilot-scale wESP system consists of five sections:

- (1) formation of sulfuric acid mist
- (2) injection of sulfuric acid mist or fine particulates
- (3) a water-supply piping system
- (4) a wet electrostatic precipitator (wESP)
- (5) aerosol measurement

A schematic diagram of the wESP system is shown in Fig. 5. To inject sulfuric acid mist, an SO₃ generator and a mist generator were used. SO₃ was generated from the reaction of SO₂ with oxygen (O₂) in a vanadium pentoxide (V₂O₅) catalyst reactor. The catalyst reactor was maintained at approximately 420°C to promote SO₃ conversion. SO₃ then interacted with water mist generated from the steam boiler to form sulfuric acid mist. The sulfuric acid mist was injected into the wESP to test its performance on the control of sulfuric acid mist. In addition, fly ash was fed from a feeder at a constant rate to test its ability to control fine particulates. A turbo fan was installed to provide a flow rate of 120 m³/min. Flushing water tanks were placed exterior to the wESP. Flushing water was supplied to the collector surface and then pumped to the water tanks through a PVC piping system, and its flow rate was controlled by an electronic valve. A wESP consists of 2 channels and 2 mechanical fields. Detailed information on the dimensions of the wESP and operating conditions are shown in Fig. 5 and Table 1.

Results and Discussion

Bench-Scale Tests

Each nozzle was tested for water distribution on the plate surface using the bench-scale system shown in Fig. 1.

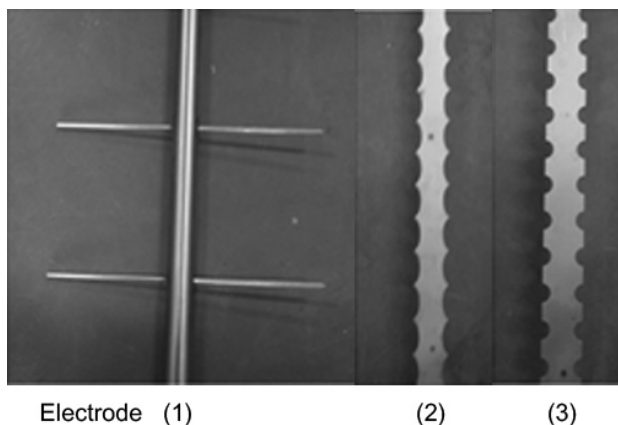


Fig. 3. Tested discharge electrodes.

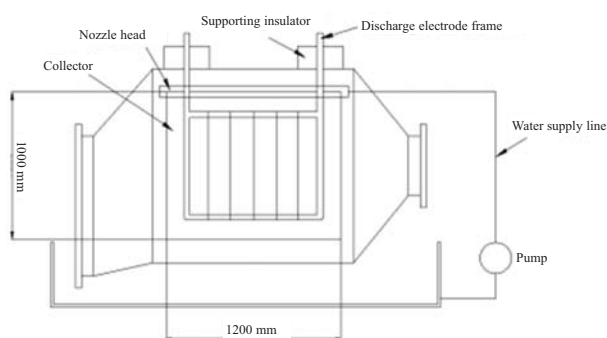


Fig. 4. Schematic of the discharge test setup.

Fig. 6 shows the water distribution when each nozzle has a varying flush rate applied. The two types of pinhole nozzles showed similar wetting patterns. Similar to the pinhole nozzles, the flat nozzle showed nonuniform water distribution by the formation of water beads on the surface. Although wetting was generally improved as the flushing rate increased, uniform distribution of flushing water was not obtained for all nozzles. To improve wetting of the plate

surface, a nanomaterial was coated on the surface. The nanomaterial liquid is commercially available (P&T-100HX, Nanopac, Korea), and its properties are shown in Table 2. The nanomaterial was coated by spraying the liquid on the plate surface, followed by drying at room temperature with heated dry air. As a result of testing with the coated plate, uniform water distribution was obtained for all nozzles (Fig. 7). It was also confirmed that this uniform water distribution was maintained after completing all tests. This shows that coating with the nanomaterial significantly improves wetting of the plate surface. Fig. 8 shows an SEM image of the plate surface after coating with the nanomaterial. Fig. 9 shows a voltage-current curve for each electrode with irrigating water. As shown here, a sharp-edged electrode (Electrode 2) and a flat-edged electrode (Electrode 3) produced higher voltage than the rod electrode with cross-arranged needles (Electrode 1) at the same current. Because an edged electrode showed effective discharge in the bench-scale tests, it was applied to the pilot-scale wESP.

Pilot-Scale Tests

Conversion of SO₂ to SO₃

The conversion efficiency of SO₂ to SO₃ in the V₂O₅ catalyst reactor was determined from the difference between the SO₂ concentrations at the inlet and outlet of the catalyst reactor. The SO₂ concentrations were measured using an SO₂ gas analyzer. As a result, the average SO₂ conversion to SO₃ was determined to be 76% (±7%). Based on this conversion efficiency, the SO₃ concentration in the inlet of wESP was assumed to be 76% of the inlet SO₂ concentration.

Wetting and Discharge Tests

Based on the bench-scale test results, pilot-scale plates were coated using the nanomaterial liquid to obtain uniform wetting of the plates. Wetting was tested with a gas velocity of 1.4–2.5 m/s and a flushing water rate of 30–70 L/min.

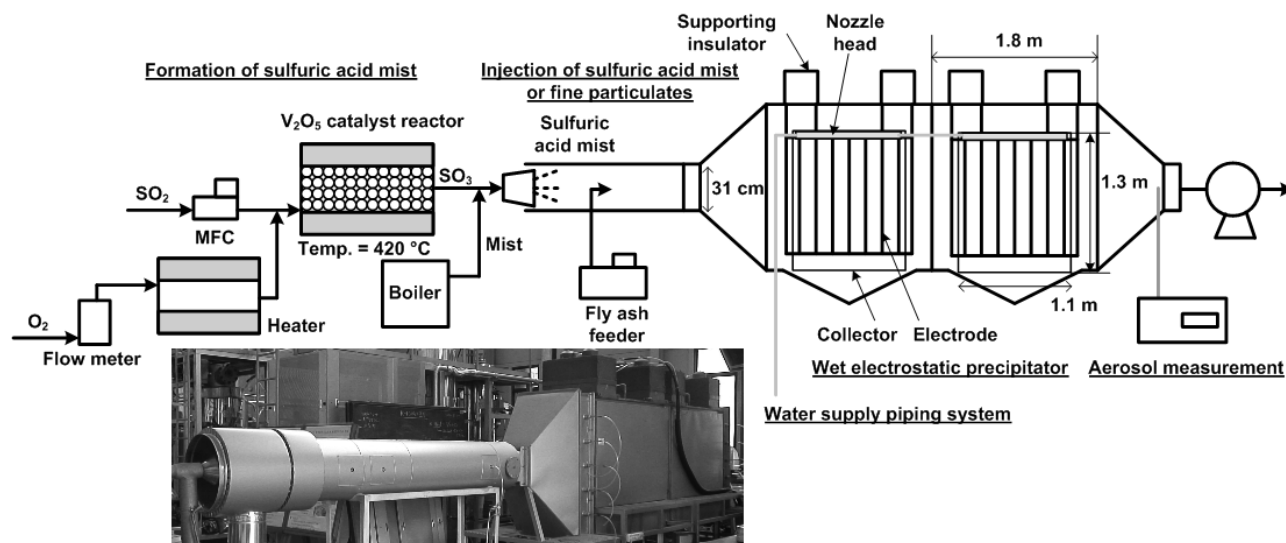


Fig. 5. Schematic of the pilot-scale wet electrostatic precipitator system.

Table 1. Summary of the experimental conditions using the pilot-scale wESP.

Item	Conditions
Height of collection plate	1.3 m
Length of collection plate	1.1 m
Duct width	0.7 m
Number of channels	2
Number of mechanical fields	2
Spray nozzle	Pressure nozzle
Gas velocity in the collector	1.4 m/sec
Flow rate of flushing water	50 L/min
Applied voltage	45, 55, and 65 kV
Inlet concentration of sulfuric acid mist (as SO ₃)	30, 50, and 100 ppm
Inlet concentration of fly ash	100 mg/Nm ³

As a result, uniform water distribution was found in all test conditions. However, generation of water mists was found in the gas flow channel when the flushing rate was more than 60 L/min. Therefore, an optimum flushing rate was determined to be 50 L/min for this wESP. Fig. 10 shows

discharge test results using the pilot-scale wESP equipped with a sharp-edged electrode. Discharge tests were conducted by increasing the flushing water rate up to 70 L/min because the applied voltage level can be lowered when mist generation occurs with an increase in the flush rate. However, similar voltage-current curves were obtained at all tested flush rates, as shown in Fig. 10. This shows that the level of discharge is consistent despite the flushing water rate increases, and that more than 60 kV is applicable with the sharp-edged electrode in the pilot-scale wESP.

Size Distribution of the Sulfuric Acid Mist and Fine Particulates

To test the collection efficiencies of the sulfuric acid mist and fine particulates, sulfuric acid mist was produced from the configuration shown in Fig. 5, and fly ash was obtained from a dry ESP located in a full-scale coal-fired power plant. The size distribution of sulfuric acid mist and fly ash was determined using an aerosol particle sizer (TSI Model 3010). The size distribution of sulfuric acid mist was measured at the inlet of the wESP and is presented in Fig. 11. As shown in the figure, sulfuric acid mist had the highest number of particles in the diameter range of 0.6~1.2 μm , and its size distribution was found to be consistent. In contrast, fly ash had the most particles at diameters of approximately 1.3 and 2.4 μm , as shown in Fig. 12. Although differences were found among three repeat-

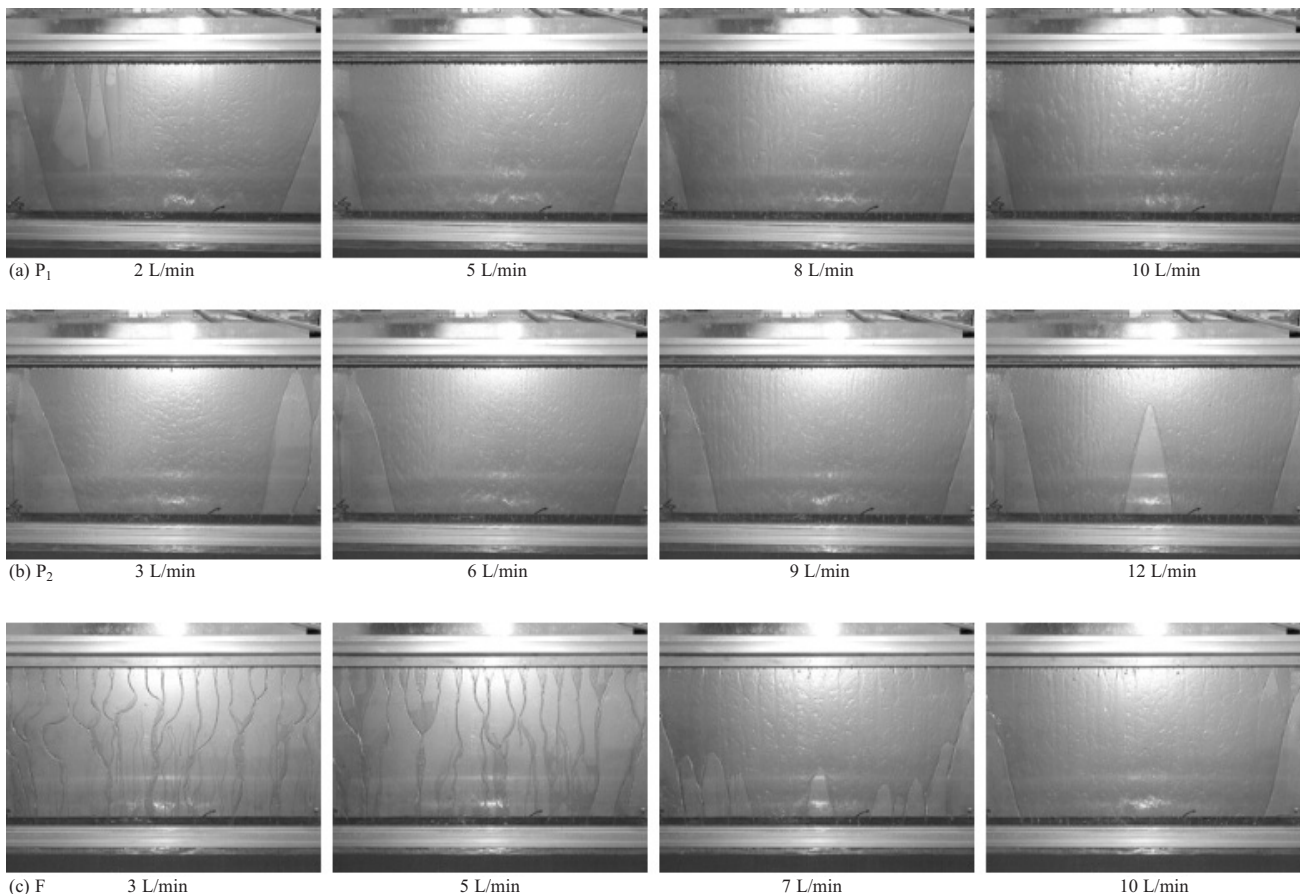


Fig. 6. Wetting characteristics of (a) pinhole nozzle type 1, (b) pinhole nozzle type 2, and (c) flat nozzle with different flush rates.

Table 2. Properties of the nanomaterial liquid used for coating.

Component (wt %)	Titanium dioxide	< 0.1
	Silica	< 5
	Ethyl alcohol	< 35
	2-Butoxyethanol	< 60
Average diameter of nanomaterial		5 nm
Wetting angle		5.09°

ed measurements of the size distribution of fly ash, the distribution trend was similar each time. Therefore, the average from these measurements was assumed to be the size distribution of fine particulates in the inlet of the wESP.

Tests on the Removal of Sulfuric Acid Mist and Fine Particulates

The pilot-scale wESP was tested for the removal of sulfuric acid mist. Fig. 13 shows collection efficiencies for each aerodynamic diameter of sulfuric acid mist when a different level of discharge is applied with an inlet SO₃ concentration of 30 ppm. Although the collection efficiency at 45 kV was relatively low, especially in the size range of 0.8~1 μm, it increased to 82~88% and 91~97% for this size range at 55 and 65 kV, respectively. In addition, the pilot-scale wESP showed 97.7%, 98.5%, and 99.3% removal efficiency at 45, 55, and 65 kV, respectively, on the basis that the mass of the particles was less than 2.5 μm in diameter (PM2.5). Similar removal efficiencies were found from the tests at the inlet SO₃ concentrations of 50 and 100 ppm. Considering that most sulfuric acid mists in coal-fired flue gases have a diameter of more than a few microns, these

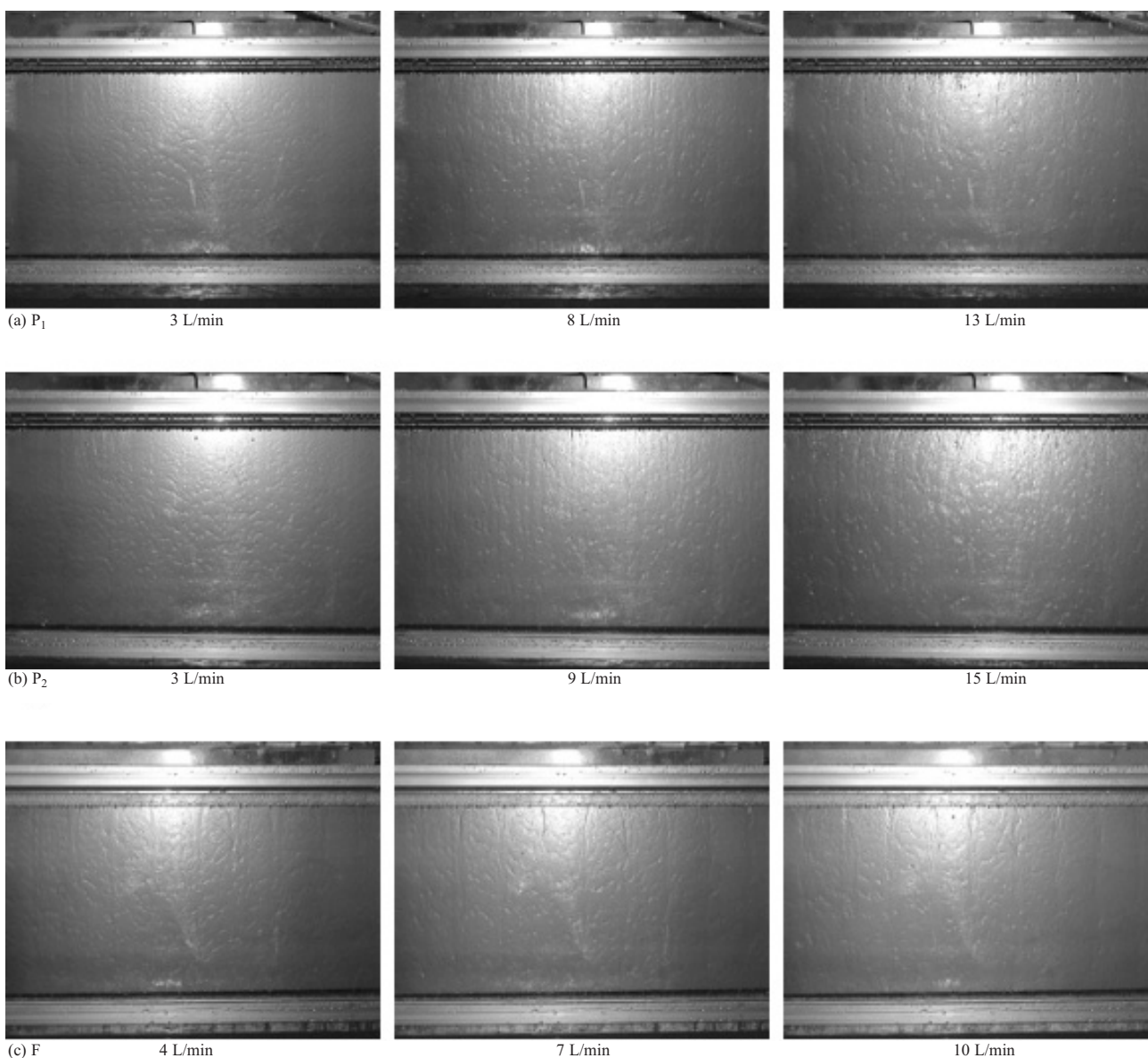


Fig. 7. Wetting characteristics of (a) pinhole nozzle type 1, (b) pinhole nozzle type 2, and (c) flat nozzle after coating the plate.

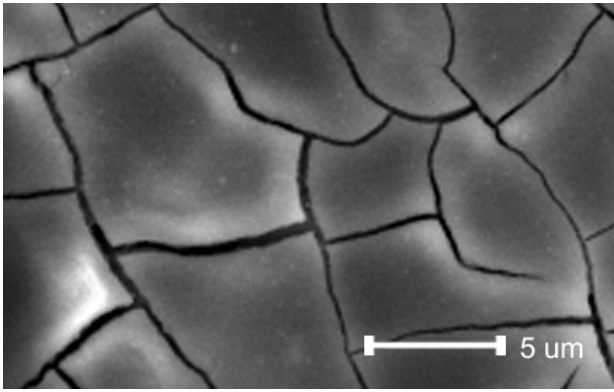


Fig. 8. SEM image of the plate surface after coating.

results show that a wESP can be a viable option for the control of sulfuric acid mist. The performance of the wESP on the control of fine particulates also was tested with several levels of discharge. Fig. 14 shows the collection efficiency for each particle size of fine particulates with applied voltages of 45, 50, 55, 60, and 65 kV. Similar to sulfuric acid mist, the lowest collection efficiency was found for particles in the size range of 0.6~1 μm. In addition, the collection efficiency increased as the applied volt-

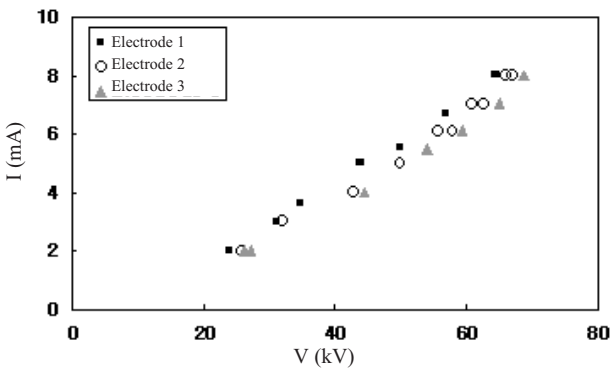


Fig. 9. Voltage-current curves for several electrodes with irrigating water.

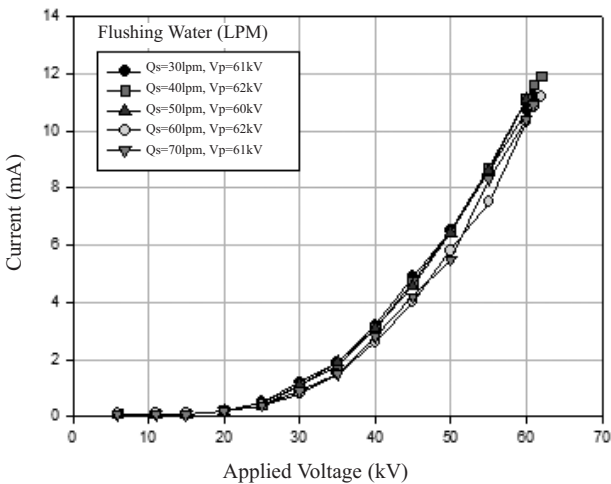


Fig. 10. Voltage-current curves at the flushing water rates applied to the pilot-scale wESP.

age increased, and the efficiency at 65 kV was approximately 96% on the basis of a mass of PM2.5. Compared with sulfuric acid mist, a lower collection efficiency was found for particle sizes around 1.3 and 2.4 μm. This may be attributed to the initial size distribution of the fly ash injected into the wESP.

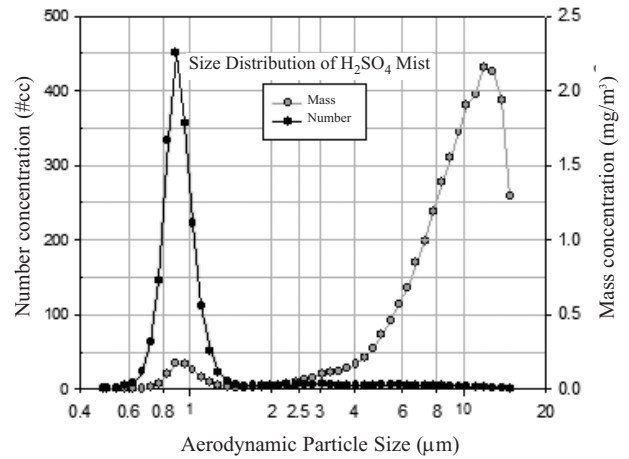


Fig. 11. Size distribution of the sulfuric acid mist produced from the generation system.

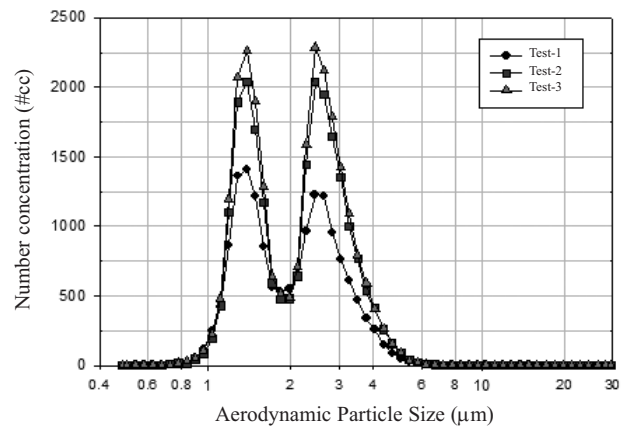


Fig. 12. Size distribution of fly ash.

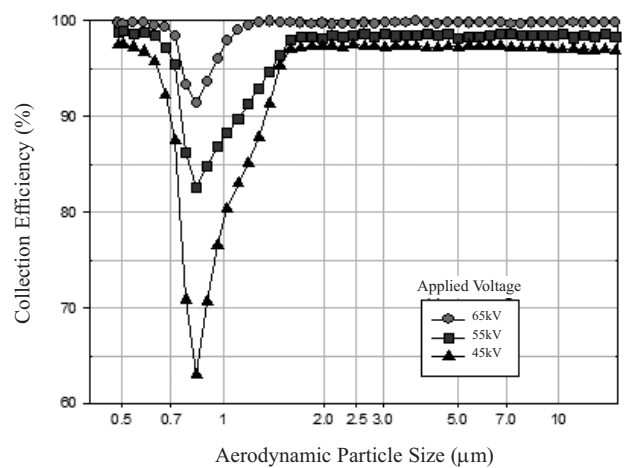


Fig. 13. Collection efficiency for the sulfuric acid mist at an inlet concentration of 30 ppm as SO₃ with applied voltages.

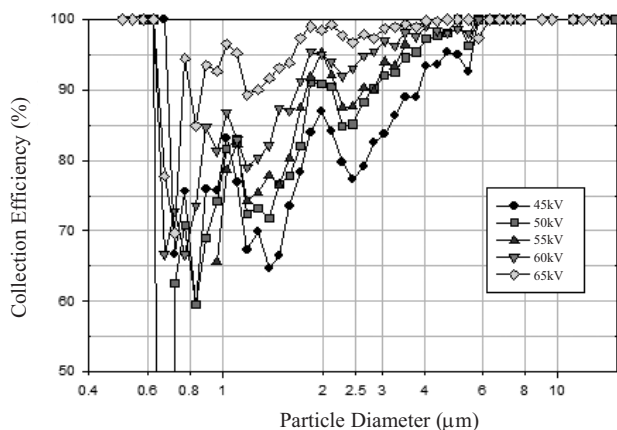


Fig. 14. Collection efficiency for particles with applied voltages.

Conclusions

To design a wet electrostatic precipitator for control of sulfuric acid mist and fine particulates, wetting of a collection plate and the discharge of electrodes were first tested using a bench-scale experimental system. For the conventional metal plate, pinhole and flat nozzles did not demonstrate uniform distribution over the plate surface. However, when the plate surface was coated with a nanomaterial, uniform water distribution was obtained over the surface with both the pinhole and flat nozzles. In the discharge tests, edged electrodes demonstrated effective discharge. These bench-scale results were applied to the design of a pilot-scale wESP. As a result, uniform water distribution over the collector surface and effective discharge were found in the pilot-scale wESP. This wESP showed more than 99% and 95% removal efficiency for PM_{2.5} of both sulfuric acid mist and fine particulates. Therefore, the pilot-scale wESP is considered to be successfully constructed to control sulfuric acid mist and fine particulates. In addition, these results show that a wESP can be used as a viable option to control sulfuric acid mist and fine particulates in combustion flue gases.

Acknowledgements

This research was supported by the Next-Generation Environmental Technology Development Project funded by Korea Ministry of the Environment.

References

1. OLEN K. R. In Acid Mist Formation in RFO-Fired Boilers and Plume Opacity Control, Conference on Formation, Distribution, Impact, and Fate of Sulfur Trioxide in Utility Flue Gas Streams, US Department of Energy-FETC, **1998**.
2. SRIVASTAVA R. K., MILLER C. A., ERICKSON C., JAMBHEKAR R. Emissions of Sulfur Trioxide from Coal-Fired Power Plants. *J. Air Waste Manage. Assoc.* **54**, (6), 750, **2004**.
3. KOZŁOWSKI R., J ŻWIĄK M., J ŻWIĄK M. A., RABAJCZYK A. Chemism of atmospheric precipitation as a consequence of air pollution: The case of Poland's holy cross mountains. *Pol. J. Environ. Stud.* **20**, (4), 919, **2011**.
4. AGENCY U. E. P. Control of Mercury Emissions from Coal-fired Electric Utility Boilers, EPA-600/R-01-109, Research Triangle Park, NC, **2002**.
5. LEVY E. K. In Effect of Boiler Operations on Sulfuric Acid Emissions, Conference on Formation, Distribution, Impact, and Fate of Sulfur Trioxide in Utility Flue Gas Streams, US Department of Energy-FETC, **1998**.
6. AHN J., OKERLUND R., FRY A., EDDINGS E. G. Sulfur trioxide formation during oxy-coal combustion. *International Journal of Greenhouse Gas Control* **5**, S127, **2011**.
7. BAYLESS D. J., SHI L., KREMER G., STUART B. J., REYNOLDS J., CAINE J. Membrane-Based Wet Electrostatic Precipitation. *J. Air Waste Manage. Assoc.* **55**, (6), 784, **2005**.
8. CHANG J., DONG Y., WANG Z., WANG P., CHEN P., MA C. Removal of sulfuric acid aerosol in a wet electrostatic precipitator with single terylene or polypropylene collection electrodes. *J. Aerosol Sci.* **42**, (8), 544, **2011**.
9. SAIYASITPANICH P., KEENER T. C., LU M., LIANG F., KHANG S. J. Control of Diesel Gaseous and Particulate Emissions with a Tube-Type Wet Electrostatic Precipitator. *J. Air Waste Manage. Assoc.* **58**, (10), 1311, **2008**.
10. DORS M., MIZERACZYK J., CZECH T., REA M. Removal of NO_x by DC and pulsed corona discharges in a wet electrostatic precipitator model. *J. Electrostat.* **45**, (1), 25, **1998**.
11. KIM J.-H., LEE H.-S., KIM H.-H., OGATA A. Electrospray with electrostatic precipitator enhances fine particles collection efficiency. *J. Electrostat.* **68**, (4), 305, **2010**.
12. TAHIR M. S., SALEEM M., MALIK S. R., KHAN J. R., SIEBENHOFER M. An innovative and advanced oxidation process for effluent treatment through wet tube-type electrostatic precipitation. *Chemical Engineering and Processing: Process Intensification* **52**, 16, **2012**.

